

NUMERICAL ANALYSIS OF TURBULENT FLOW OVER A BACKWARD-FACING STEP USING REYNOLDS STRESS CLOSURE MODEL

Jung Yul Yoo*, Hae Cheon Choi* and Sang Myeong Han*

(Received March 7, 1989)

Reynolds stress turbulence models are adopted and applied for calculating turbulent flow over a backward-facing step. For the diffusion term in the transport equations for the Reynolds stresses, two gradient-type models are employed and compared. In addition, investigations on the modified ϵ equations are carried out. The results of the computations are compared with the extant experimental data. As a consequence, it is concluded that the Reynolds stress models predict the flow field better than the standard $k-\epsilon$ model in the recirculating region. However, after the reattachment the return to the ordinary turbulent boundary layer is shown to be too slow to predict the flow field irrespective of turbulence models.

Key Words: Reynolds Stress Closure Model, Modified ϵ Equations, Backward-Facing Step

1. INTRODUCTION

Separation and reattachment of turbulent flow are important processes in many engineering applications, including diffusers, airfoils with separation bubbles, heat exchangers, and combustors. The turbulent flow over a backward-facing step is among the simplest that can display these processes. Although there have been many researches in this field, our current understanding of the reattachment process is still lacking because, despite the simplicity of the configuration, the flowfield is very complex, i.e., it consists of three zones such as recirculating region, reattaching region and redeveloping region.

Eaton and Johnston(1981) reviewed the general features of the backward-facing step flow. The separated shear layer appears to be much like an ordinary plane-mixing layer through the first half of the separated flow region. But the reattaching shear layer differs from the plane-mixing layer in the sense that the flow on the low-speed side of the shear layer is highly turbulent, as opposed to the low turbulence level stream in a typical plane-mixing layer experiment.

Bradshaw and Wong(1972) measured turbulence quantities in the reattachment and redeveloping regions. They indicated that shear stress and turbulence length scale in the reattachment region decrease spectacularly, mainly because of the confinement of the large eddies by the solid surface. And many researchers(Bradshaw and Wong, 1972; Kim et al., 1978; Chandrsuda and Bradshaw, 1981) reported the dip in the velocity profile near reattachment which persists for a downstream distance of about fifty step heights. The persistence of the dip implies that turbulence is not in local equilibrium and the length scale of the turbulence is not proportional to y , i.e., $l = ky$ but increases much more rapidly with y .

When flow separation occurs, turbulence structure

becomes more complicated so that the theoretical study on turbulent separated flow becomes more difficult. Among the existing turbulence models, the Reynolds Stress Model, which provides transport equations for the Reynolds stresses, can explain anisotropic characteristics of turbulent diffusion while the standard $k-\epsilon$ model cannot. This model has been systematically developed and improved by several researchers(Rotta, 1951; Daly and Harlow, 1970; Hanjalic and Launder, 1972; Launder et al., 1975).

In this study, the Reynolds stress closure model suggested by Launder et al.(1975) is applied to turbulent flow over a backward-facing step. To account for the fluctuating pressure field by the presence of the wall, the pressure-containing correlation model proposed by Gibson and Launder(1978) is also applied. The results are compared with the experimental data(Kim et al., 1978) and also partly with the standard $k-\epsilon$ model.

2. GOVERNING EQUATIONS

The continuity and momentum equations describing the turbulent flow considered in the present study are of steady two-dimensional form as follows:

$$\frac{\partial}{\partial x_j}(\rho U_j) = 0, \quad (1)$$

$$\frac{\partial}{\partial x_j}(\rho U_i U_j) = -\frac{\partial p}{\partial x_i} + \frac{\partial}{\partial x_j} \left[\mu \left(\frac{\partial U_i}{\partial x_j} + \frac{\partial U_j}{\partial x_i} \right) - \rho \overline{u_i u_j} \right], \quad (2)$$

2.1 Reynolds Stress Model(RSM)

We write the transport equations for the Reynolds stresses as

$$\frac{\partial}{\partial x_k}(\rho \overline{u_i u_j}) = P_{ij} - \epsilon_{ij} + \phi_{ij} + \phi_{ij,w} + D_{ij}, \quad (3)$$

where,

*Department of Mechanical Engineering, Seoul National University, Seoul 151-742, Korea

$$P_{ij} = -\left(\overline{u_j u_k} \frac{\partial U_i}{\partial x_k} + \overline{u_i u_k} \frac{\partial U_j}{\partial x_k}\right) : \text{generation}, \quad (4)$$

$$\epsilon_{ij} = 2\nu \frac{\partial u_i}{\partial x_k} \frac{\partial u_j}{\partial x_k} : \text{dissipation}, \quad (5)$$

$$\phi_{ij} = \frac{p}{\rho} \left(\frac{\partial u_i}{\partial x_j} + \frac{\partial u_j}{\partial x_i} \right) : \text{pressure-strain correlation}, \quad (6)$$

$\phi_{ij,w}$ = pressure-strain correlation with a near-wall correction,

$$D_{ij} = -\frac{\partial}{\partial x_k} (\overline{u_i u_j u_k}) : \text{diffusion}. \quad (7)^*$$

Equation (5) is readily modelled by the well-known form given by Rotta(1951):

$$\epsilon_{ij} = \frac{2}{3} \delta_{ij} \epsilon. \quad (8)$$

The pressure-strain term (6) is expressed by combining Rotta's linear return-to-isotropy hypothesis and the linear approximation of Launder et al.(1975),

$$\begin{aligned} \phi_{ij} = & -C_1 \frac{\epsilon}{k} (\overline{u_i u_j} - \frac{2}{3} \delta_{ij} k) - \frac{C_2 + 8}{11} (P_{ij} - \frac{2}{3} \delta_{ij} P) \\ & - \frac{30C_2 - 2}{55} k \left(\frac{\partial U_i}{\partial x_j} + \frac{\partial U_j}{\partial x_i} \right) \\ & - \frac{8C_2 - 2}{11} (Q_{ij} - \frac{2}{3} \delta_{ij} P), \end{aligned} \quad (9)$$

where $C_1 = 1.5$, $C_2 = 0.4$,

$$\begin{aligned} Q_{ij} = & -\overline{u_i u_k} \frac{\partial U_k}{\partial x_j} - \overline{u_j u_k} \frac{\partial U_k}{\partial x_i}, \\ P = & -\overline{u_i u_j} \frac{\partial U_i}{\partial x_j}. \end{aligned}$$

In order to approximate the term $\phi_{ij,w}$, Amano and Goel(1985) simply adopted Launder et al.(1975)'s model. However, in the present study, we adopt Gibson and Launder(1978)'s model which allows the proximity of a rigid wall to modify the pressure field and thus impedes the transfer of energy from the streamwise direction to that normal to the wall:

$$\phi_{ij,w} = \phi_{ij,w_1} + \phi_{ij,w_2}, \quad (10)$$

with

$$\begin{aligned} \phi_{ij,w_1} = & C_1' \frac{\epsilon}{k} (\overline{u_k u_m n_k n_m} \delta_{ij} - \frac{3}{2} \overline{u_k u_i n_k n_j} \\ & - \frac{3}{2} \overline{u_k u_j n_k n_i}) f\left(\frac{l}{n_i r_i}\right), \end{aligned}$$

$$\begin{aligned} \phi_{ij,w_2} = & C_2' (\phi_{km,2} n_k n_m \delta_{ij} - \frac{3}{2} \phi_{ik,2} n_k n_j \\ & - \frac{3}{2} \phi_{jk,2} n_k n_i) f\left(\frac{l}{n_i r_i}\right), \end{aligned}$$

$$\phi_{ij,2} = -C_\phi (P_{ij} - \frac{2}{3} \delta_{ij} P),$$

where \underline{r} is the position vector, l is a characteristic turbulence length scale, $C_1' = 0.5$, $C_2' = 0.3$ and $C_\phi = 0.6$. The function $f\left(\frac{l}{n_i r_i}\right)$ is expressed as

$$f\left(\frac{l}{n_i r_i}\right) = \frac{C_\mu^{3/4} k^{3/2}}{k \epsilon n_i r_i},$$

where $C_\mu = 0.09$ and $k = 0.4187$.

It was suggested by Daly and Harlow(1970) that the diffu-

* Only diffusion by turbulent velocity fluctuations is retained, while diffusion by molecular interaction and pressure-induced diffusion are neglected(Launder et al.(1975)).

sion rate (7) may be evaluated as

$$D_{ij} = C_s \frac{\partial}{\partial x_k} \left(\frac{k}{\epsilon} \overline{u_k u_i} \frac{\partial u_j}{\partial x_i} \right), \quad (11)$$

where $C_s = 0.25$.

A more complex and seemingly superior model for this diffusion term was developed by severe simplification of the exact transportation equation [Launder et al.(1975)] as follows:

$$\begin{aligned} D_{ij} = & C_s \frac{\partial}{\partial x_k} \left[\frac{k}{\epsilon} \left(\overline{u_i u_i} \frac{\partial u_j u_k}{\partial x_i} + \overline{u_j u_i} \frac{\partial u_k u_i}{\partial x_i} \right. \right. \\ & \left. \left. + \overline{u_k u_i} \frac{\partial u_i u_j}{\partial x_i} \right) \right], \end{aligned} \quad (12)$$

where $C_s = 0.11$.

2.2 Transport Equation for Turbulence Energy Dissipation Rate

The transport equation for ϵ used in the high Reynolds number form of the $k-\epsilon$ model is given as

$$\frac{\partial}{\partial x_j} (\rho U_j \epsilon) = \rho \frac{\epsilon}{k} (C_{\epsilon_1} P - C_{\epsilon_2} \epsilon) + \frac{\partial}{\partial x_j} \left[\left(\mu + \frac{\mu_t}{\sigma_\epsilon} \right) \frac{\partial \epsilon}{\partial x_j} \right], \quad (13)$$

where the Boussinesq's eddy-viscosity concept is employed to express the production term P and $\mu_t = C_\mu \rho k^2 / \epsilon$ is the turbulent viscosity. In fact, Amano and Goel(1985) used this form of the transport equation for ϵ together with the transport equations for Reynolds stresses which are quite similar to those given in the previous subsection except the expression for $\phi_{ij,w}$.

Instead, in the present study, we adopt the form of the transport equation for ϵ which was developed and used in Hanjalic and Launder(1972):

$$\frac{\partial}{\partial x_j} (\rho U_j \epsilon) = \rho \frac{\epsilon}{k} (C_{\epsilon_1} P - C_{\epsilon_2} \epsilon) + C_\epsilon \frac{\partial}{\partial x_j} \left(\rho \frac{k}{\epsilon} \overline{u_i u_j} \frac{\partial \epsilon}{\partial x_i} \right). \quad (14)$$

The values of the constants used in the transport equations for ϵ are as follows:

$$\begin{aligned} C_{\epsilon_1} = & 1.44, \quad C_{\epsilon_2} = 1.92 \text{ [for Eq.(13)] or } 1.90 \text{ [for Eq.(14)]} \\ \text{and } \sigma_\epsilon = & 1.22. \end{aligned}$$

For comparison, we also consider Sinder's modification of the production term in the ϵ equation which resulted in a marked improvement for some flow problems(Launder et al., 1981):

$$P = -\overline{u_i u_j} \frac{\partial U_i}{\partial x_j} = \frac{\mu_t}{\rho} \frac{\partial U_i}{\partial x_j} \frac{\partial U_i}{\partial x_j}. \quad (15)$$

3. NUMERICAL METHOD

For the calculation of the flow field a modified version of the TEACH-2E code(Gosman and Ideriah, 1976) has been devised, which is compatible with the turbulence models described above and the necessary boundary conditions. The control volumes for mean-velocity components are the stag-

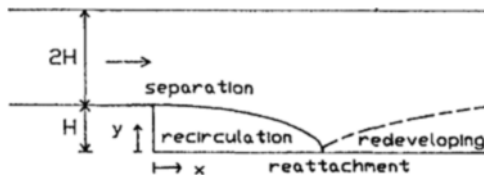


Fig. 1 Flow domain

gered systems in which the locations of U_1 and U_2 are shifted half-cell distances in the x_1 and x_2 directions, respectively. All of the normal Reynolds stresses $\overline{u_i^2}$ are calculated at the scalar node points along with P , k , and ϵ , while the shear Reynolds stress $\overline{u_1 u_2}$ is calculated at the southwest corner of the scalar cell. The convective terms appearing in the transport equations are all approximated by hybrid scheme. More detailed derivation of the discretized equations may be found in Han(1987).

Schematic diagram of the flow domain is shown in Fig. 1. At the inlet, all quantities are specified according to the experimental condition(Kim et al., 1978) and the fully developed condition. At the outlet, the Neumann condition are used. At the wall boundaries, the law of the wall is used for the velocities and the turbulent quantities. Particularly, the boundary conditions for the Reynolds stresses are precisely the same as those used by Launder, Reece and Rodi(1975). For example, at the horizontal walls,

$$\begin{aligned} \overline{u_1^2} &= 5.1 u_\tau^2, \\ \overline{u_2^2} &= 1.0 u_\tau^2, \\ \overline{u_3^2} &= 2.3 u_\tau^2, \\ \frac{\partial \overline{u_1 u_2}}{\partial x_2} &= 0, \end{aligned}$$

where u_τ is the friction velocity and the coefficients in the normal stresses represent a consensus of several of the most thoroughly documented wall flows.

Computations are performed on a 42×42 non-uniform grid system with an expansion factor of 1.07 in the x -direction. The criteria of convergence has been a maximum residual source of the mass flow rate or momentum below 0.05%.

4. RESULTS AND DISCUSSIONS

The results of the computation were mainly compared with the data of Kim et al.(1978).

4.1 Reattachment Length (x_r)

The most important factor to be looked for in comparing the numerical results with the experimental results for the flow over a backward facing step is the reattachment length, x_r . Numerous attempts have been made to fit x_r to the extant experimental results with turbulence models (Eaton, 1981; Amano and Goel, 1985).

The mean reattachment distance obtained by the experiment of Kim et al.(1978) was found to be $x_r/H = 7 \pm 1$. In Table 1, the reattachment lengths by different turbulence models are listed. Generally speaking, it can be said that RSM predicts x_r better than $k-\epsilon$. However, contrary to our expectations, the use of the invariant form of the diffusion term (12) did not give a much better result than the use of simple diffusion term (11). Regarding the transport equation

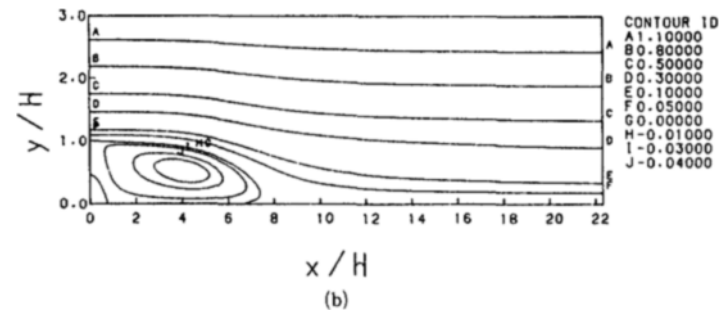
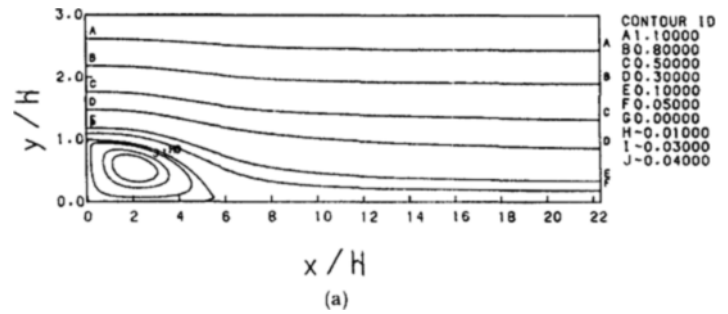


Fig. 2 Streamlines : (a) $k-\epsilon$ model ; (b) RSM

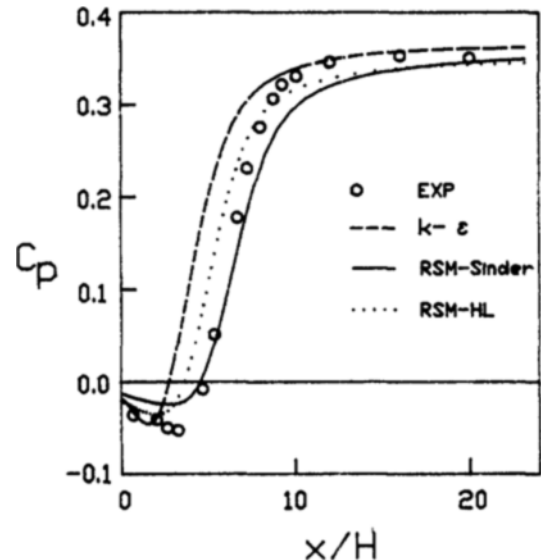


Fig. 3 Step-side pressure distributions

for ϵ , it was reported in 1980-1981 AFOSR-HTTM-STANFORD Conference(Launder et al., 1981) that Eq.(14) did not give good results due to the presence of the production term. And in the simulation of round jet by Launder and Morse(1977), it was also reported that RSM with the use of Eq.(14) gave worse results than standard $k-\epsilon$ model. The similar results are shown in our computation. It seems that Sinder's work (Eq.(15)) which modified the production term in ϵ equation approaches the experimental results.

Streamlines obtained by using $k-\epsilon$ model and RSM are shown in Fig. 2. The RSM shows the turbulence-driven secondary flow in salient corner while $k-\epsilon$ model does not. The C_p curves obtained by using different models are compared in Fig. 3.

4.2 Local Mean Velocity and Turbulent Quantities

Figure 4 shows the local mean streamwise velocity profiles at different locations. In recirculating region, RSM predicts the mean velocity better than $k-\epsilon$ model. In redeveloping region, the results by $k-\epsilon$ model and RSM-HL are more similar to the experimental data. This is considered to be only due to the fact that they predict shorter reattachment distances than can be observed in the experiment. At $x/H=16$, the experimental results reveal the characteristics of the turbulent boundary layer while the numerical results do not. Clearly, the flow structure after reattachment predicted by the numerical calculation returns to ordinary turbulent boundary layer at a much slower rate than in the experiment.

The turbulent kinetic energy is shown in Fig. 5. The under-prediction of the reattachment length in most numerical calculations may be explained by the over-prediction of the turbulent kinetic energy. More specifically, while $k-\epsilon$ model and RSM-HL overpredict the turbulent kinetic energy in the recirculating region, RSM-Sinder predicts better resulting in

larger numbers of x_R in Table 1. After reattachment, the values of the turbulent kinetic energy may be irrelevant to turbulence models.

The behaviors of the turbulent intensity is quite similar to those of the turbulent kinetic energy, as shown in Fig. 6. Especially, the maximum turbulent intensities, irrespective of turbulence models, are nearly the same as the experimental results after reattachment. But at $x/H=16$, the numerical results underpredict the turbulent intensity near wall because of the slow return to the ordinary turbulent boundary layer. Figure 7 shows the Reynolds shear stress. Generally, it can be said that the shear stress distributions are successfully predicted by the Reynolds stress model with Sinder's modification.

4.3 Further Remarks

The algorithm for present computation is based on hybrid scheme. When the turbulent Reynolds stresses are included in the momentum equation as source terms, the accuracy of the

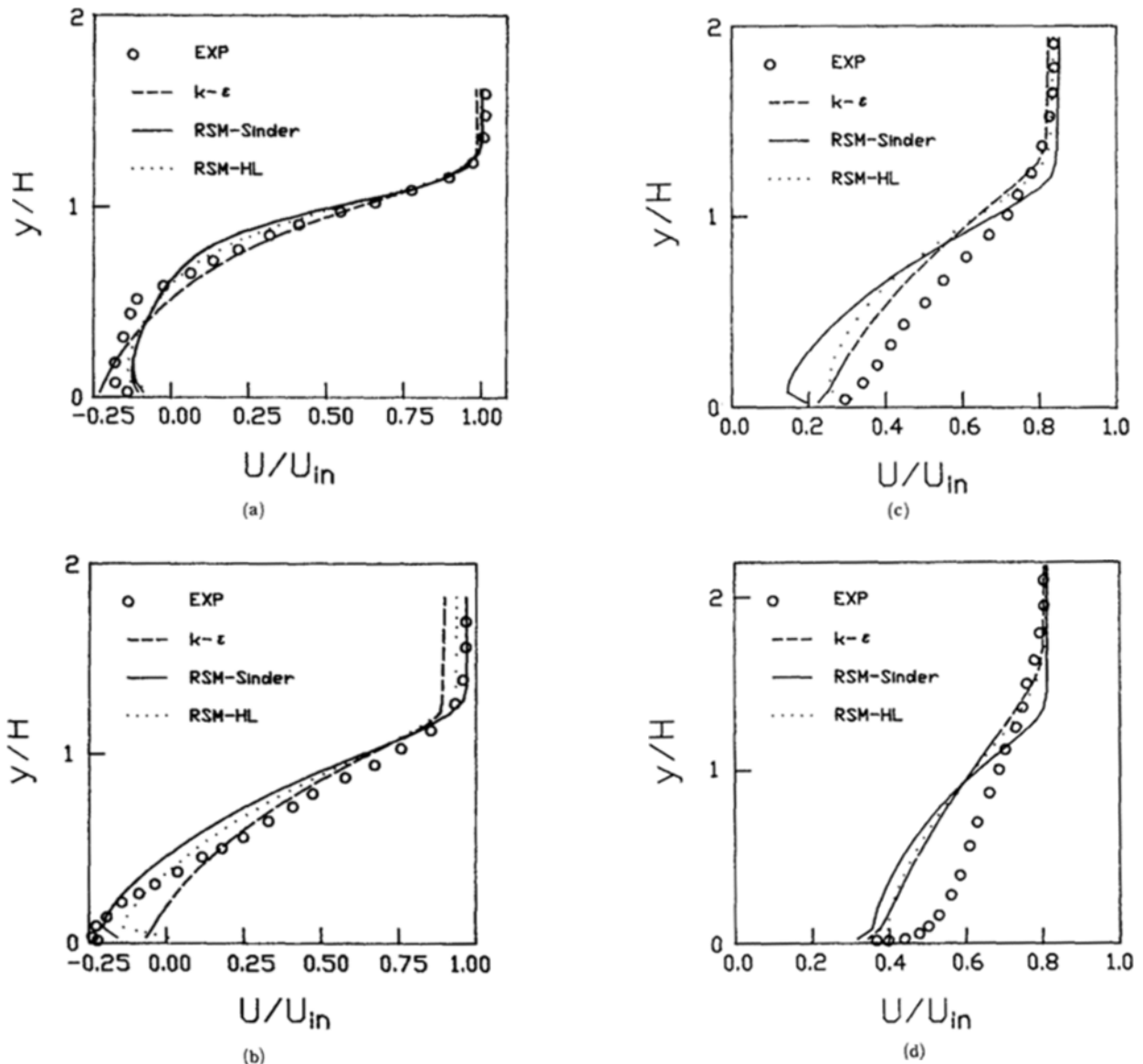


Fig. 4 Mean streamwise velocity profile at $x/H =$ (a) 2.67; (b) 5.33; (c) 9.78; (d) 16.

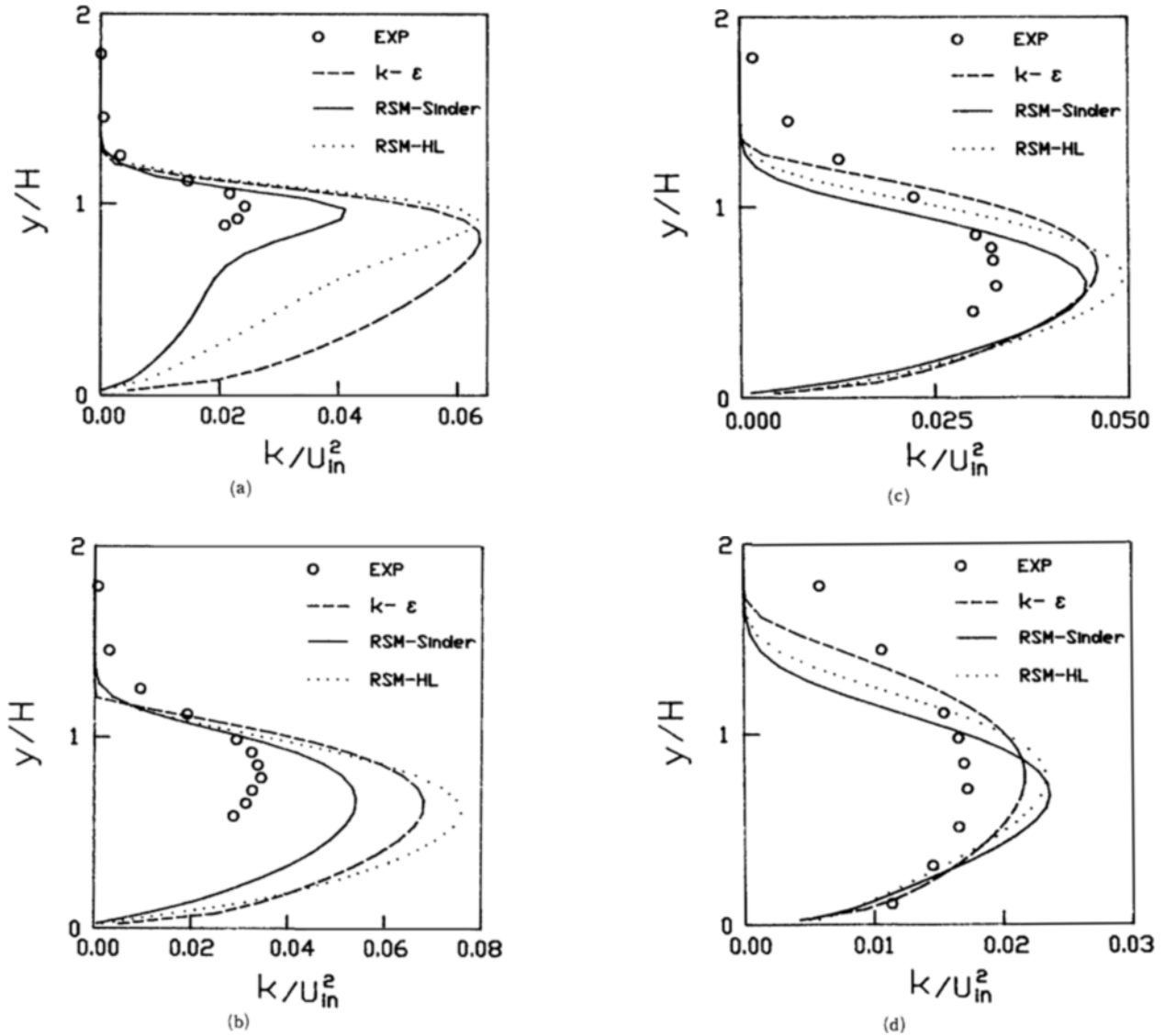


Fig. 5 Turbulent kinetic energy at $x/H =$ (a) 2.33 ; (b) 5.887 ; (c) 8.553 ; (d) 15.667 (In the experimental results, k is approximated by $\frac{3}{4}(\overline{u^2} + \overline{v^2})$)

Table 1 Reattachment lengths for different turbulence models

k eq. or Reynolds stress eqs.	ϵ eq.	x_R/H	Remark
k eq.	Eq.(13)	5.51	Standard $k-\epsilon$
Eqs.(3)-(10), (11)	Eq.(13)	6.90	
	Eq.(14)	4.81	
	Eqs.(14)-(15)	6.97	
Eqs.(3)-(10), (12)	Eq.(13)	7.10	RSM-HL RSM-Sinder
	Eq.(14)	4.15	
	Eqs.(14)-(15)	7.10	

computation may fall to first-order in some regions of flow domain. It is noteworthy that the upwind corrected scheme adopted by Choi et al.(1988) can be applied to this case to assure the second-order accurate solutions.

The use of the law of wall in near-wall grid cannot be

justified because of the dip in the velocity profile after reattachment as stated in INTRODUCTION. Moreover, the use of zero-flux condition for the turbulent Reynolds stresses (Celenigil and Mellor, 1985; Tahry, 1985) may create some nonphysical solutions. Therefore, more researches on wall-boundary conditions are required in numerical simulation of the flow with steep pressure gradients, i.e., step wall in this case.

5. CONCLUSIONS

A numerical simulation of the turbulent flow over a backward-facing step using Reynolds stress models has been performed.

It is shown that RSM with ϵ equation modified by Sinder(RSM-Sinder) predicts the reattachment length better than $k-\epsilon$ model and RSM with ϵ equation modified by Hanjalic and Launder(RSM-HL).

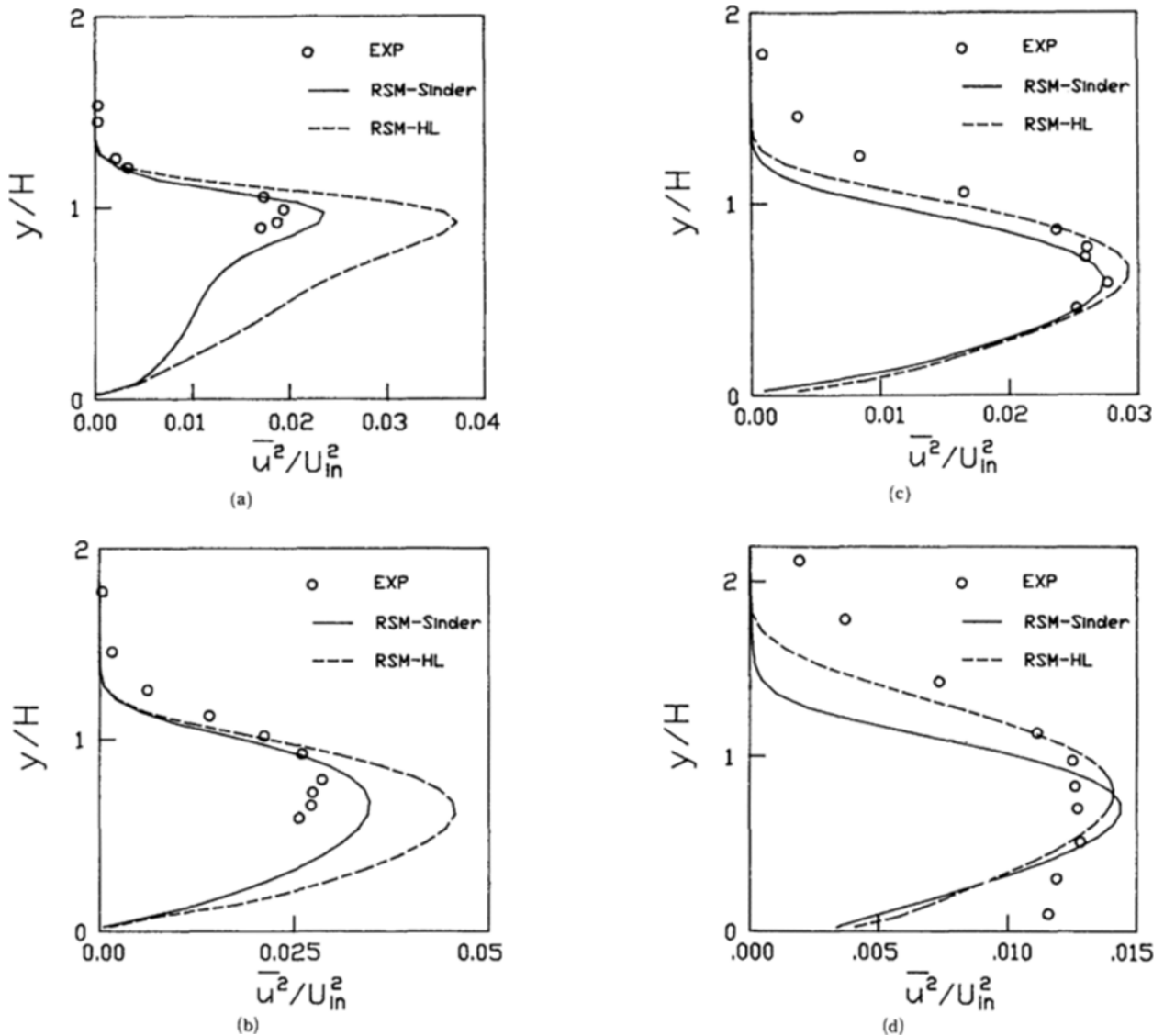


Fig. 6 Turbulent intensity at $x/H =$ (a) 2.33 ; (b) 5.887 ; (c) 8.553 ; (d) 15.667

The profiles of the mean velocity and the turbulent quantities using RSM-Sinder are closer to the experimental data than those using standard $k-\epsilon$ and RSM-HL. But it is shown that the very slow return to the ordinary turbulent boundary layer after reattachment makes far downstream flow field reveal the characteristics of plane mixing layer as opposed to the experimental results. Last but not least, it is required that the wall-boundary conditions should be thoroughly studied in the region after reattachment where the dips in the velocity profile occur.

ACKNOWLEDGEMENT

The authors gratefully acknowledge the full support of this research by the Korea Science and Engineering Foundation.

REFERENCES

- Amano, R.S. and Goel, P., 1985, "Computations of Turbulent Flow Beyond Backward-Facing Steps Using Reynolds Stress Closure", *AIAA J.*, Vol. 23, No. 9, pp. 1356~1361.
- Bradshaw, P. and Wong, F.Y.F., 1972, "The Reattachment and Relaxation of a Turbulent Shear Layer", *J. Fluid Mech.*, Vol. 52, part 1, pp. 113~135.
- Celenligil, M.C. and Mellor, G.L., 1985, "Numerical Solution of Two-Dimensional Turbulent Separated Flows Using a Reynolds Stress Closure Model", *J. Fluids Eng.*, Vol. 107, pp. 467~476.
- Chandrsuda, C. and Bradshaw, P., 1981, "Turbulence Structure of a Reattaching Mixing Layer", *J. Fluid Mech.*, Vol. 110, pp. 171~194.
- Choi, H.C., Song, J.H. and Yoo, J.Y., 1988, "Numerical Simulation of the Planar Contraction Flow of a Giesekus Fluid", *J. Non-Newtonian Fluid Mech.*, Vol. 29, pp. 347~379.
- Daly, B.J. and Harlow, F.H., 1970, "Transport Equations in Turbulence", *Physics of Fluids*, Vol. 13, No. 11, pp. 2634~2649.
- Eaton, J.K. and Johnston, J.P., 1981, "A Review of Research on Subsonic Turbulent Flow Reattachment", *AIAA J.*, Vol. 19, No. 9, pp. 1093~1100.
- Eaton, J.K., 1981, "Incompressible Separated Flows-

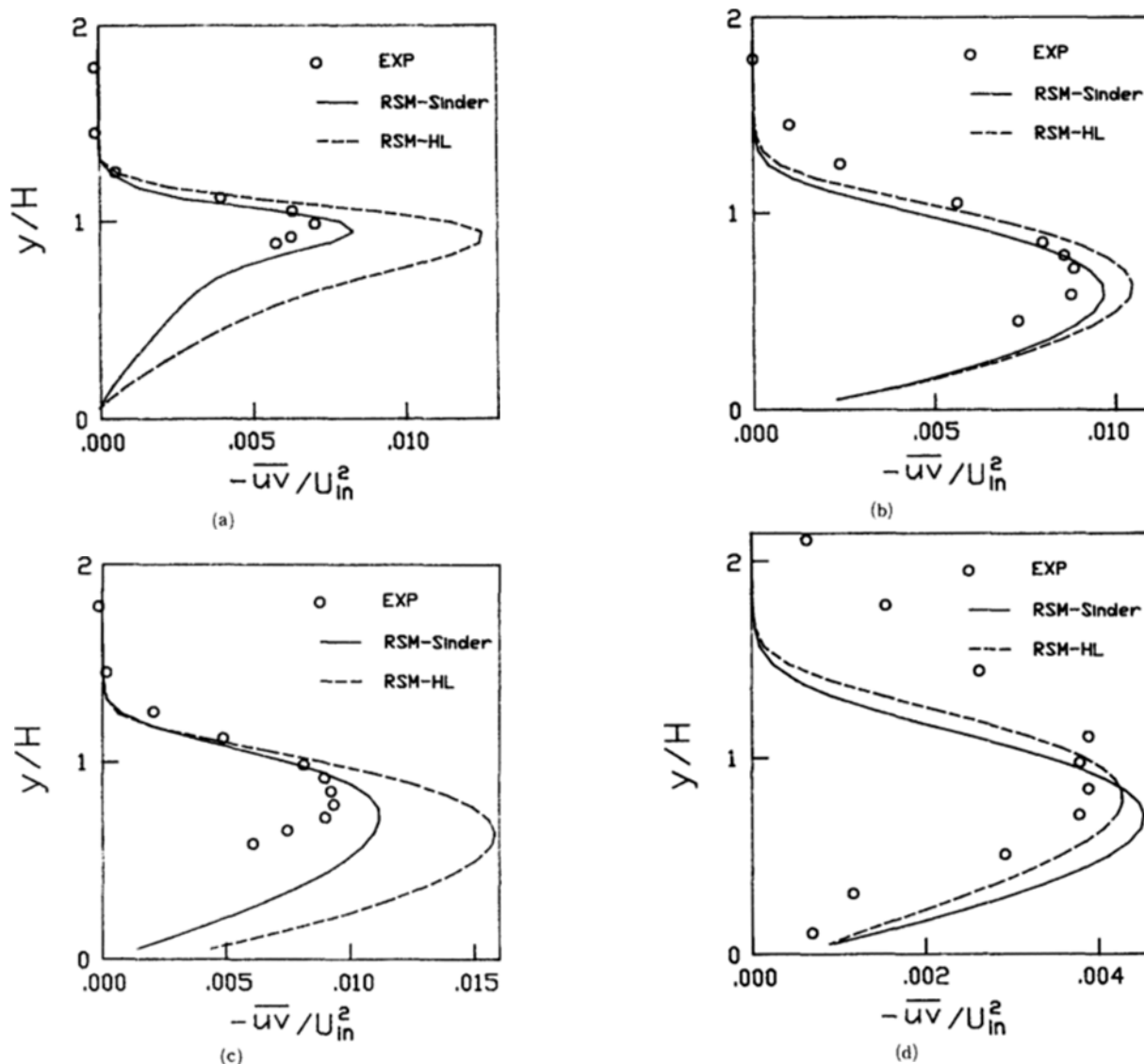


Fig. 7 Reynolds shear stress at $x/H =$ (a) 2.33 ; (b) 5.887 ; (c) 8.553 ; (d) 15.667

Internal Flows : Backward-Facing Step”, 1980-81 AFSOR-HTTM-STANFORD Conference on Complex Turbulent Flows : Taxonomies, Reporter’s Summaries, Evaluation and Conclusions, Stanford University, Stanford, Calif.

Gibson, M. M. and Launder, B.E., 1978, “Ground Effects on Pressure Fluctuations in the Atmospheric Boundary Layer”, *J. Fluid Mech.*, Vol. 86, part 3, pp. 491~511.

Gosman, A.D. and Ideriah, F.J.K., 1976, “TEACH-2E : A General Computer Program for Two-Dimensional, Turbulent, Recirculating Flows”.

Han, Sang Myeong., 1987, “Numerical Analysis of Turbulent Flow with Recirculating Region”, M.S. Thesis, Dept. of Mechanical Engineering, Seoul National University.

Hanjalic, K. and Launder B.E., 1972, “A Reynolds Stress Model of Turbulence and Its Application to Thin Shear Flows”, *J. Fluid Mech.*, Vol. 52, part 4, pp. 609~638.

Kim, J., and Kline, S.J. and Johnston, J.P., 1978, “Investigation of Separation and Reattachment of a Turbulent Shear Layer : Flow over a Backward-Facing Step”, MD-37, Thermosciences Division, Dept. of Mechanical Engineering, Stanford University.

Launder, B.E., Reece, G.J. and Rodi, W., 1975, “Progress in the Development of a Reynolds-Stress Turbulence Closure”, *J. Fluid Mech.*, Vol. 68, part 3, pp. 537~566.

Launder, B.E. and Morse, A., 1977, “Numerical Prediction of Axisymmetric Free Shear Flows with a Reynolds Stress Closure”, *Turbulent Shear Flows I*, Springer-Verlag, Berlin, pp. 279~294.

Launder, B.E., Leschziner, M.A. and Sinder, M., 1981, “Comparison of Computation with Experiment : Summary Report”, 1980~81 AFOSR-HTTM-STANFORD Conference on Complex Turbulent Flows : Comparison of Computation with Experiment and Computers’ Summary Reports, Stanford University, Stanford, Calif.

Rotta, J.C., 1951, “Statistische Theorie Nichthomogener Turbulenz”, *Zeitschrift für Physik*, Vol. 129, pp. 547~572.

Shir, C.C., 1973, “A Preliminary Numerical Study of Atmospheric Turbulent Flows in the Idealized Planetary Boundary Layer”, *J. Atmos. Sci.*, Vol. 30, pp. 1327~1339.

Tahry, S.E., 1985, “Application of a Reynolds Stress Model to Engine-Like Flow Calculations”, *J. Fluids Eng.*, Vol. 107, pp. 444~450.